Combustion and Flame 203 (2019) 265–278

Contents lists available at ScienceDirect

Combustion and Flame

journal homepage: www.elsevier.com/locate/combustflame

Measurement of the reaction rate of $H + O_2 + M \rightarrow HO_2 + M$, for M= Ar, N_2, CO_2, at high temperature with a sensitive OH absorption diagnostic

Rishav Choudhary, Julian J. Girard, Yuzhe Peng, Jiankun Shao*, David F. Davidson, Ronald K. Hanson

Department of Mechanical Engineering, Stanford University, 418 Panama Mall, Room 104, Stanford, CA 94305-3032, USA

ARTICLE INFO

Article history:
Received 22 November 2018
Revised 19 January 2019
Accepted 15 February 2019

Keywords:
Chemical kinetics
Laser diagnostics
Shock tube
OH absorption
Reaction rate

ABSTRACT

The reaction rate of $H + O_2 + M = HO_2 + M$ in the low-pressure limit was determined in the temperature range of 1450– 2000 K, with Argon, Nitrogen, and Carbon Dioxide as the third-body collision partners, by measuring the OH time-history after the induction time during lean oxidation of Hydrogen. Test conditions were optimized to suppress the sensitivity of OH to interfering reactions after the induction time, using dilute and extremely lean mixtures at these temperatures. The strong $Q_1(5)$ transition in the A-X(0,0) band of OH was used as the probing wavelength for the diagnostic. Calibration measurements were performed prior to the experiments to estimate the effects of pressure shift and collision broadening on the absorption coefficient of OH for each of the bath gas species, which enabled a reduction in the uncertainty in the absorption cross-section of OH. Aided by the calibrated and improved OH diagnostic, the reaction rate constants were determined at high temperatures, with low scatter, and tight uncertainty bounds. The measured rate constants also agree with the extrapolation of previous investigations at lower temperatures. Combined rate constant expressions based on the lower temperature measurements of Shao et al. (2018) and the current high-temperature measurements are proposed, which are valid over the temperature range of 1000–2000 K:

$$k_{2,Ar} = \left(2.66 * 10^{19}\right) * T^{-1.36}\ \mathrm{cm^6 mol^{-2} s^{-1}}\ (\pm 9\ \%)$$

$$k_{2,N_2} = \left(2.25 * 10^{21}\right) * T^{-1.95}\ \mathrm{cm^6 mol^{-2} s^{-1}} (\pm 23\%)$$

$$k_{2,CO_2} = \left(2.23 * 10^{18}\right) * T^{-0.79}\ \mathrm{cm^6 mol^{-2} s^{-1}} (\pm 28\%)$$

1. Introduction

As the norms for acceptable levels of emission from power-generation systems and automobiles are becoming progressively stringent, so is the need for cleaner and more efficient combustion systems that can help in achieving those targets. A better understanding of the kinetics of fuels used in these combustion systems is a key step towards achieving this target. Additionally, with increasing interest towards the development of advanced propulsion systems like scramjets, the need for improving the existing knowledge of the kinetics of oxidation of fuels is imperative. This need has catalyzed the development of numerous kinetic mechanisms in the recent past [1–5].

Improvement in the accuracy of the mechanisms is intimately linked with the accuracy of the constitutive reactions. This emphasizes the need for improved measurements of key reactions in the mechanisms. For Hydrogen, and smaller hydrocarbons, the reactions:

$$H + O_2 = OH + O \quad (R1)$$

$$H + O_2 + M = HO_2 + M \quad (R2)$$

play particularly important roles in determining ignition, extinction, and flame speeds. R1 is endothermic, strongly temperature dependent, a primary chain-branching pathway, and is widely regarded as one of the most important reactions in high temperature combustion chemistry. R2 is an exothermic, weakly temperature-dependent reaction, which serves as the primary chain termination pathway in a certain temperature range. The competition between

* Corresponding author.
E-mail address: jkshao@stanford.edu (J. Shao).

https://doi.org/10.1016/j.combustflame.2019.02.017
0010-2180/

these two pathways strongly dictates the conditions of ignition, extinction, and flame speeds.

The need for tighter uncertainty bounds on the rate constant of R1 and R2 was highlighted by Tao et al. [6] To identify the critical remaining uncertainties in the recently proposed chemical kinetic mechanism FFCM-1, they evaluated the prediction uncertainties in the extinction and ignition residence times over a wide range of operating conditions in a perfectly-stirred reactor with methane as the fuel. They noted that in order to attain a prediction uncertainty of less than 20%, it is imperative to reduce the uncertainty in R1 and R2 to less than 20%.

The rate constant of R1 is already well known, owing to the recent investigations of Hong et al. [7] and Wang et al. [8]. However, significant uncertainties persist in the knowledge of the rate constant of R2. Moreover, most of the high-temperature measurements of this reaction were taken in a very narrow temperature range (1000–1400 K). The previous studies have either used ignition delay time measurements [9,10], or leveraged the time-history of species during the recombination phase of oxidation to estimate $k_{2,Ar}$ [11–13]. Some of the studies also relied on measurement of NO_2 in diluted Hydrogen and Oxygen mixtures, perturbed by the addition of nitric oxide. [14–17]

Global phenomena like ignition delay time measurements can be used in some cases to infer the rate constants of reactions of interest. Mertens et al. [10] determined the rate constant of R2 for $M = N_2$, Ar, and H_2O by adjusting its value in a detailed chemical kinetics model to match ignition delay times for $H_2/CO/O_2/N_2$, $H_2/CO/O_2/Ar$, and $H_2/CO/O_2/N_2/H_2O$ mixtures with fuel/air equivalence ratios of $\phi = 0.5$, 0.9, and 1.0. The most recent study undertaken by our group, prior to this work, followed a similar approach [9]. That study was performed behind reflected shocks in the High-Pressure Shock Tube (HPST) facility at Stanford, in the temperature range of 1150–1300 K, between 17 atm and 33 atm, and it resulted in a significant reduction in the uncertainty of $k_{2,M}$, for four different bath gases, i.e. Ar, N_2, H_2O, and CO_2. The conditions for the experiments were chosen such that the ignition delay times showed a high sensitivity to R2, which resulted in a determination of the rate constant of R2 with tight uncertainty bounds. This method was also successful in reducing the scatter of data, albeit over a very narrow temperature range.

Getzinger et al. [11] studied the recombination phase of stoichiometric, lean, and rich Hydrogen-Oxygen mixtures in the temperature range of 1100–1700 K, and pressures between 0.5 atm and 5 atm, in a shock tube. Using their simplified hypothesis of partial equilibrium of the recombination reactions, their model gave a satisfactory estimate for the reaction rate constants, when used with the OH time-history measured using ultraviolet laser absorbance. In another study, Getzinger et al. [12] measured the time history of water formed during oxidation, using an IR emission-based diagnostic, and used similar equilibrium arguments to estimate the rate constant of the title reaction. This last study was performed over a wide temperature range, but the significant scatter in these results emphasizes the need for further investigation.

Addition of NO to Hydrogen/Oxygen mixtures at high temperatures is known to alter the kinetics. The termination product, HO_2, can be consumed by NO to form NO_2 and OH through R3. This reaction is fast, and leads to a build-up of NO_2, which is quickly consumed by R4 to re-generate NO and OH.

$$HO_2 + NO = NO_2 + OH \quad (R3)$$

$$NO_2 + H = NO + OH \quad (R4)$$

Using the steady-state assumption for HO_2 and NO_2 gives a simplified expression for $k_{2,M}$, and can be expressed as $k_{2,M} = k_4[NO_2]_{ss}/[O_2]$. Thus, measurement of plateau values of NO_2 using laser absorbance in $H_2/O_2/NO$ systems can be used to estimate $k_{2,M}$. This idea has been leveraged by several investigators in the past. While Bromly et al. [14], Ashman and Haynes [15], and Mueller et al. [16] measured the reaction rate constant in a temperature range of 700–900 K using flow reactors, Bates et al. [17] pushed the domain of knowledge further by making reliable measurements behind reflected shocks in the temperature range of 1050–1250 K, over a pressure range of 7–152 atm, with Ar, N_2, and H_2O as the collision partners. Despite being an improvement over the previous measurements, the uncertainty in the quoted measurements was high, and covered a very narrow temperature range. Fernandes et al. [18] measured the rate constants in the pressure range of 1.5–950 bar, albeit at lower temperatures (300–900 K), with Ar, N_2, and He as the collision partners.

The only reported measurements at higher temperatures, as discussed earlier, exhibit a significant scatter; this highlights the need for further studies of the rate constant of R2 at higher temperatures. Recognizing this need, we report in this paper our recent measurements of $k_{2,M}$ in the temperature range of 1450–2000 K, and in the pressure range of 10–22 atm, with Ar, N_2, and CO_2 as the third-body collision partners. Our experiments were designed based on our observation that at extremely lean conditions ($\Phi = 0.025$), the decay profile of OH is exclusively sensitive to the title reaction. The recent development of improved frequency-doubling crystals has enabled access to the Q-branch transitions of the A-X(0,0) band of OH, which owing to their higher line-strength, has enabled accurate ppm level detection of OH radicals [19]. Probing the OH radicals using this powerful OH diagnostic helped to reduce the overall uncertainty in the measured rate constant.

2. Experimental setup

2.1. Selection of the test conditions

The dominance of chain-branching reactions over termination reactions prior to ignition leads to a rapid build-up of H, O, OH, and HO_2 radicals, which upon ignition are slowly consumed by termolecular recombination reactions. Under extremely lean conditions, the high concentration of residual Oxygen molecules makes R2 one of the most important recombination reactions. The recombination product, HO_2, is further consumed through a series of fast bimolecular reactions (R5-R9) to form OH.

$$HO_2 + H = 2OH \quad (R5)$$

$$HO_2 + H = O + H_2O \quad (R6)$$

$$O + H_2O = 2OH \quad (R7)$$

$$HO_2 + O = OH + O_2 \quad (R8)$$

$$HO_2 + OH = H_2O + O_2 \quad (R9)$$

These fast reactions coupled with the fact that R2 is the primary source of HO_2 radicals, ensure that this recombination reaction has the dominant controlling effect on the rate at which the OH radical population approaches equilibrium. This is demonstrated by a formal sensitivity analysis of the OH time-history shown in Fig. 1. Here, sensitivity to the reaction rate constant k_i is defined as $S_i(t) = (\Delta[OH](t)\ /[OH](t))/(\Delta k_i/k_i)$. The simulations were performed using CHEMKIN-PRO, with FFCM-1 [20] as the reference mechanism. The OH radical concentration shows an exclusive sensitivity to R2 for over 800 microseconds during its decay phase for one of the test conditions. Also shown in Fig. 1 is the simulated OH time-history at the same conditions with the unmodified mechanism. Furthermore, the OH time-history obtained

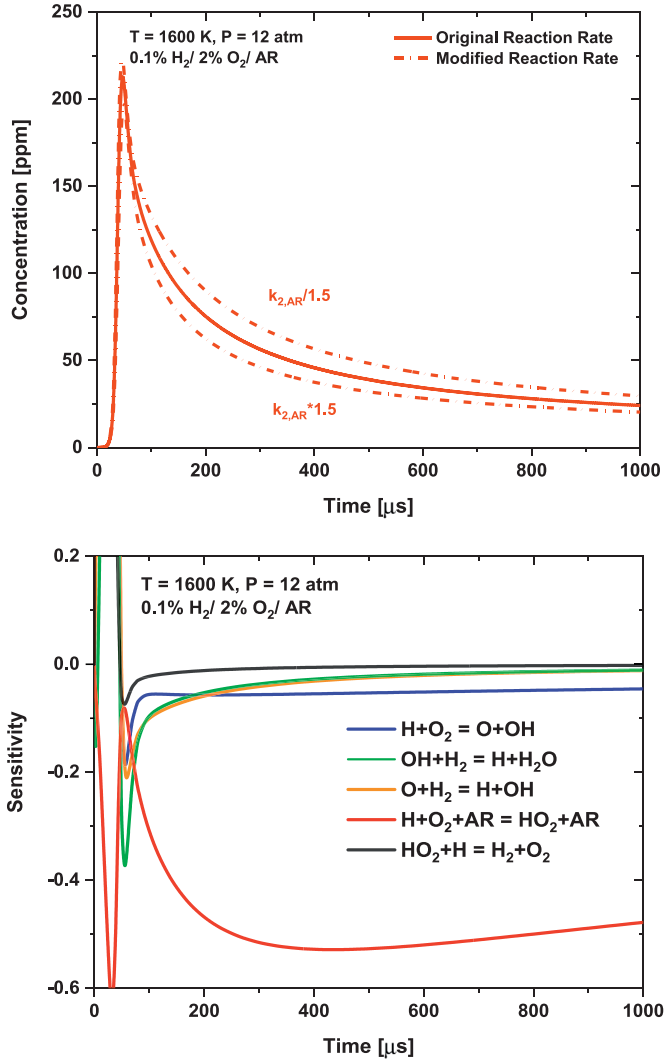

Fig. 1. (Top) Simulated time-history of OH during lean oxidation of Hydrogen heavily diluted in Argon. (Bottom) OH sensitivity for the corresponding test condition. Both figures illustrate that the time-history of OH is dominantly sensitive to R2.

by perturbing the rate constant of R2 by the quoted uncertainty factor of 1.5 is shown on the same plot, which demonstrates the high-sensitivity of OH time-history to R2. Thus, fitting a simulated OH time-history to the measured OH time-history can lead to a reasonably accurate determination of the rate constant of R2.

The dominance of sensitivity of the OH concentration to R2 extends over a wide temperature range from 1450 K to 2100 K in the pressure range of 8–30 atm for lean Hydrogen-Oxygen mixtures ($\Phi < 0.04$), with Argon and Nitrogen as the diluents. Similar sensitivity is also shown in mixtures with CO_2 as the diluent. Although R10 becomes increasingly important at higher concentrations of CO_2, adjusting the CO_2 concentration in the mixture can suppress the sensitivity of OH to R10.

$$CO+OH=H+CO_2 \quad \text{(R10)}$$

For the experiments performed in this study, the initial fuel loading was adjusted to ensure that the concentration of OH radicals produced during the test was sufficient to a achieve a high SNR measurement, but to also have only a small temperature and pressure rise after ignition of less than 1%. It should be noted that R2 is a pressure-dependent reaction, for which the high-pressure limit at elevated temperatures is reached at pressures in excess of

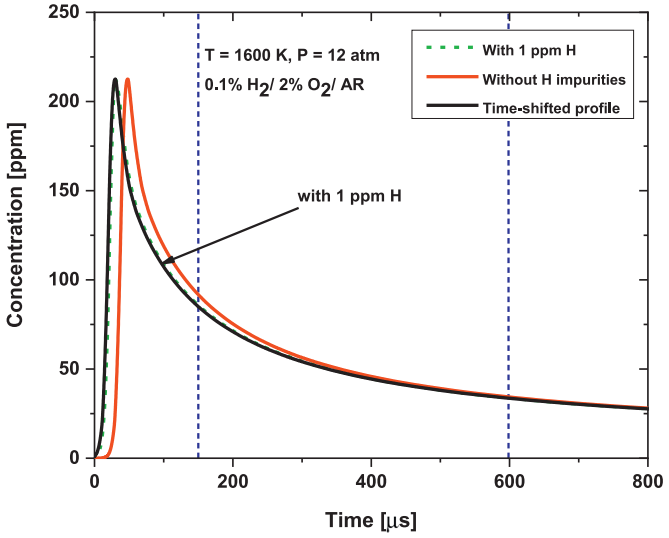

Fig. 2. Impact of impurities on the OH time-history. Time-shifting the red trace to match the induction time leads to an exact match with the green trace. (For interpretation of the references to color in this figure legend, the reader is referred to the web version of this article.)

1000 atm. Following the pressure dependence suggested by Troe [21], the reaction rate at pressures chosen for this study (8–13 atm) differs by ~1% from its low-pressure limit, which is lower than the quoted uncertainty in the current study. Thus, no correction in the estimated rates is required to account for pressure. Sellevag et al. [22] suggested a falloff factor for Nitrogen and Argon that is slightly higher than that of Troe. Calculations with their rate expressions also confirms that R2 does not enter the falloff regime at the chosen test conditions. Hong et al. [23] compared the pressure dependence suggested by Sellvag et al., Bates et al., and Fernandes et al., and noted that falloff effects below 80 atm are negligible at temperatures higher than 1000 K.

In order to test the sensitivity of the OH decay profile to impurities, simulations were also performed with addition of 1 ppm of H radicals to the test mixture over the domain of experimental conditions. 1 ppm is the upper limit of the typical H-equivalent impurity levels in this shock tube at 2000 K [24]. As can be seen from Fig. 2, the presence of impurities only affects the induction time, while the decay profile is unaffected. This is an advantage of this method over alternative methods that rely on the measurement of ignition delay time, which are usually sensitive to impurity levels in the shock tube.

2.2. HPST facility

The experiments were performed using the Stanford high-purity, High-Pressure Shock Tube (HPST). The stainless-steel driven section has an internal diameter of 5 cm and was heated to 90 °C. Diaphragms were made of aluminum (with cross-scribing of different depths) to allow measurements over a broad range of pressure. In this facility, typical uniform test times were of the order of 1 ms when helium was used as the driver gas.

The facility has been used extensively for high-pressure kinetics studies [25–28]. High-purity Hydrogen, Oxygen, Nitrogen, and Carbon Dioxide gases were supplied by Praxair™. Gas mixtures were prepared manometrically in a 12.8-liter stainless-steel mixing tank at 110 °C, and mixtures were stirred using a magnetically-driven vane assembly for at least 15 min prior to each experiment. A sidewall-mounted Kistler™ PZT, 1.1 cm away from the shock tube end wall, provided pressure time-histories. Additionally, five PCB pressure transducers were mounted at fixed locations

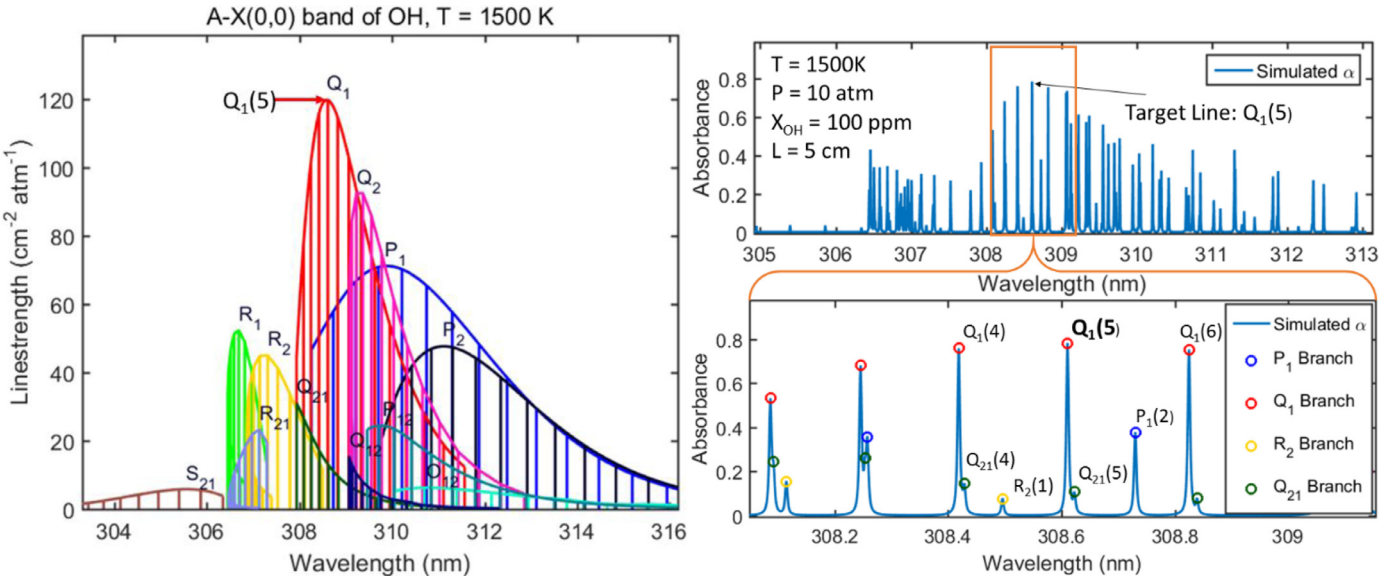

Fig. 3. (Left) Simulated line-survey of A-X(0,0) band, spectral data provided by Goldman et al. [41]; note that $Q_1(5)$ is the strongest line at T = 1500 K. (Right) Simulated absorbance for given conditions, with zoom of the spectral region immediately surrounding the line of interest below.

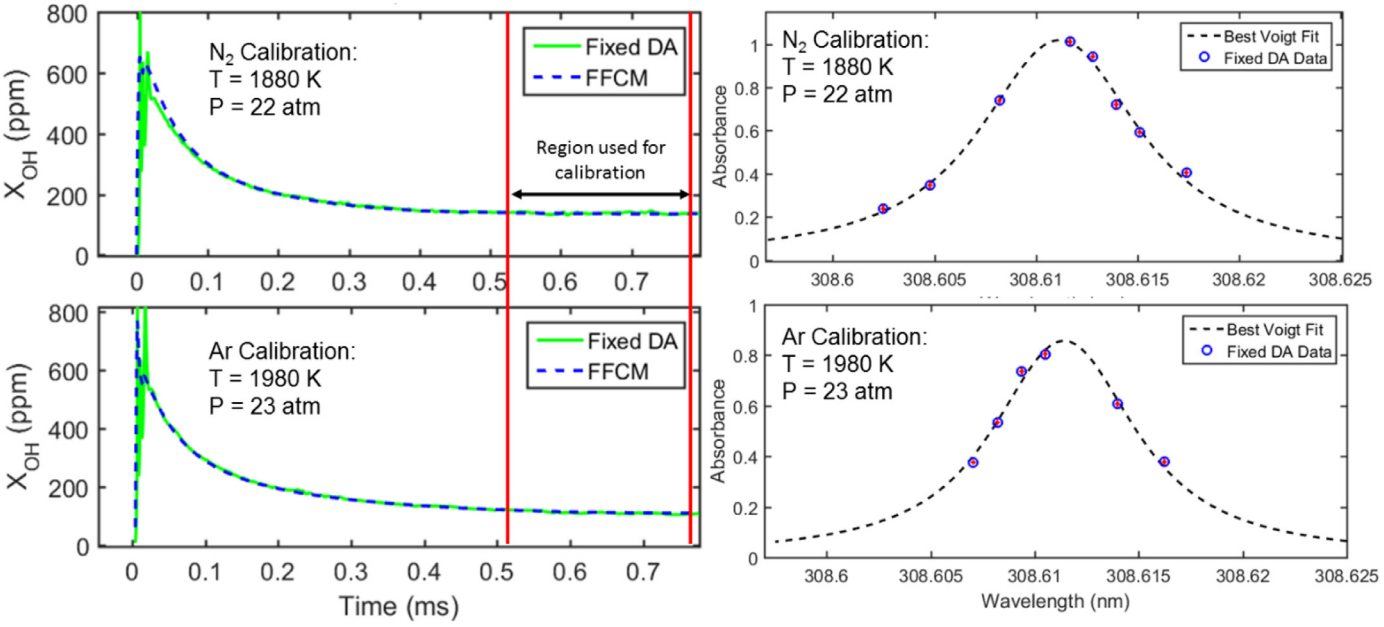

Fig. 4. (Left) Typical OH time-histories used for the N_2 and Ar lineshape characterizations (above and below respectively), with plateau region of interest indicated by vertical bounds. (Right) Characterization absorbance data plotted with 1-σ vertical and horizontal error and the associated optimized Voigt fit. The particular wavelengths chosen were highly stable modes for the dye laser resonator and ensured optimal wavelength resolution.

along the driven section. The time-history of pressure recorded by each of the pressure transducers was used to ascertain the time of arrival of the incident shock at the respective locations of the PCBs. This information was used to calculate the incident shock velocity at each of these locations, the extrapolation of which was used to obtain the shock velocity at the end-wall. The incident shock velocity at the end-wall, along with the state and the composition of the test gas mixture provided inputs to an in-house code, FROSH (based on a model that employs fundamental shock relations [29]), to obtain the temperature and pressure behind the reflected shock. There is less than ±1% uncertainty in the calculated initial reflected-shock temperature and pressure.

2.3. OH diagnostic

Fixed-wavelength direct-absorption (fixed-DA) spectroscopy, utilizing the $Q_1(5)$ transition in the A-X(0,0) band of OH, was used in this study to measure OH concentrations within the reflected-shock region of the HPST facility. Incident (I_0) and transmitted (I_t) measured signals were converted to OH mole-fraction through the Beer-Lambert relation, expressed here for a specific wavelength and transition, assuming uniform conditions along the absorbing path-length:

$$\alpha_\nu = -\ln\left(\frac{I_t}{I_0}\right)_\nu = S_{OH}(T)PX_{OH}L\Phi_\nu \qquad (1)$$

Table 1
Calibrated spectroscopic parameters. 2γ and δ referenced to $T_0 = 2000$ K. S values for the current study correspond to the Ar-broadened and N_2-broaded data sets, respectively. (a) Girard et al. [31]; (b) Wang et al. [19]; (c) Shirinzadeh et al. [43].

Broadening partner	$2\gamma_{\text{OH-B}}$ [cm^{-1}/atm]	$\delta_{\text{OH-B}}$ [cm^{-1}/atm]
[a]Ar	0.035 ± 0.003	−0.008 ± 0.001
[b]Ar	0.034 ± 0.005	−0.010 ± 0.0025
[a]N_2	0.049 ± 0.004	−0.0075 ± 0.001
[a]CO_2	0.063 ± 0.003	−0.0085 ± 0.001
[c]O_2	0.036 ± 0.008	−0.006 ± 0.001

Study	$S(T_0 = 2000\,\text{K})$ [cm^{-2}/atm]
Wang et al. [18]	71.5 ± 2.5
Current study	70.7 ± 2.1; 71.9 ± 2.6
Suggested value	71.4 ± 1.8

Table 2
Spectroscopic uncertainty sources and their corresponding contributions to the measured OH mole fraction.

Source of uncertainty:	Temperature	$\gamma_{\text{OH-B}}$	$\delta_{\text{OH-B}}$	S_0	ν_{laser}
% of measured X_{OH}	0.5%	1.3%	0.25%	1.25%	0.3%

For the given absorbing path-length, L, with pressure known using side-wall transducer measurements and the temperature deduced from the measured incident shock velocity via FROSH, only the linestrength at a reference temperature T_0, $S_{OH}(T_0)$, and lineshape function, Φ_ν, must be known to infer X_{OH} from fixed-wavelength absorption data [30]. For this study, the lineshape function was assumed to conform to the two-parameter Voigt distribution. This assumption is supported by the work of Wang et al. [19] and Girard et al. [31], which utilized fixed-DA measurements from the $Q_1(5)$ transition of OH at relatively lower pressures.

To fully characterize the lineshape function at the given experimental conditions, the collisional broadening ($2\gamma_{\text{OH-B}}$) and pressure-shift ($\delta_{\text{OH-A}}$) coefficients for all mixture components (denoted as B) with respect to the absorbing molecule (OH) must be known. This study involved several collision partners/diluents (i.e. Ar, N_2, O_2, CO_2), necessitating measurement of these spectroscopic parameters before the rate-constant study could be conducted. Considering the direct impact of measured OH concentration uncertainty on the extrapolated rate constant error, measurement precision was taken as a priority. The line selection process and subsequent spectroscopic calibration are discussed in the following sections.

2.3.1. Line selection & experimental configuration

The A-X(0,0) rovibronic band of OH has been targeted frequently in past studies requiring sensitive OH detection in combustion applications [32–35]. Previous work to characterize spectral parameters of transitions within the A-X(0,0) band for such applications was often limited to the R_1 branch and band-head region [36–40] due to frequency-doubling limitations that have since been overcome with advances in solid-state laser and second-harmonic generation technologies.

The $Q_1(5)$ line was specifically selected within the A-X(0,0) rovibronic band of OH for this application in consideration of its optimal strength and adequate spectral isolation at the conditions of interest (Fig. 3). The $Q_{21}(5)$ line interferes with the low-frequency wing of the $Q_1(5)$ transition, though it contributes negligibly toward the measured absorbance at the line-center wavelength chosen for this study.

To probe the OH $Q_1(5)$ transition in the HPST facility, spectrally narrow (negligible width) tunable laser light at the wavelength of interest was provided by a SpectraPhysics 380 series ring dye laser. The 1f light at ~ 617 nm was doubled by a critically phase-matched LBO crystal, and the 2f UV output, with a typical power of ~ 1 mW, was collimated and directed towards the HPST facility where it was split and directed onto a reference and absorption detector, both Newport model 2032 large-area UV photodetectors. A Bristol 771 high-resolution spectrum analyzer with a wavelength resolution of ~ 0.006 cm^{-1} was used to ensure single-mode lasing and operation at the linecenter wavelength. Narrow bandgap filters and spatial filters were used to prevent emission from corrupting the detector signal. The lineshape selection process and experimental set-up are detailed more extensively by Girard et al. [31].

2.3.2. Spectroscopic calibration

The scarcity of published data regarding important lineshape parameters of Q_1-branch transitions necessitated an in-house characterization for all relevant molecular broadening partners. Quantitative fixed-DA measurements require precise knowledge of $S_{OH}(T_0)$, $2\gamma_{\text{OH-X}}$, and $\delta_{\text{OH-X}}$ (e.g. X = Ar, N_2, CO_2 and O_2). Highly lean oxidation of propane in mixtures with 5–10% Oxygen and 90–95% broadening partner of interest provided an optimal calibration condition, forming a plateau concentration of OH whose

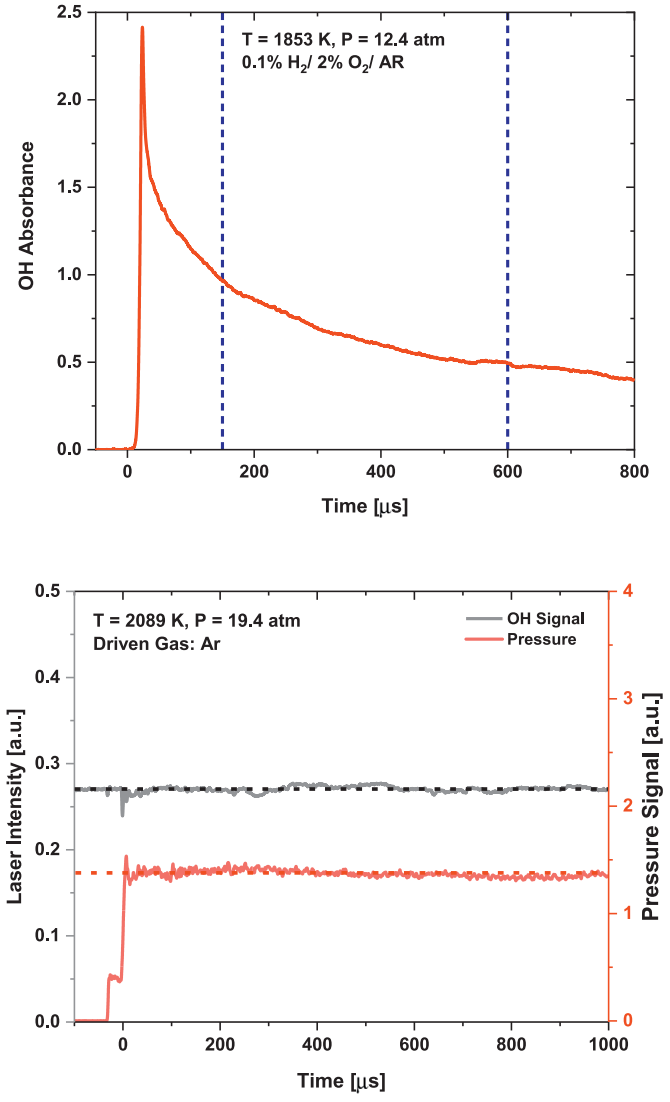

Fig. 5. (Top) Raw OH absorbance trace measured at an initial temperature and pressure of 1853 K, 12.4 atm respectively, for the test mixture 0.1% H_2/ O_2/ Ar. The blue dashed lines represent the fitting interval. (Bottom) Laser and pressure trace from a non-reacting experiment. (For interpretation of the references to color in this figure legend, the reader is referred to the web version of this article.)

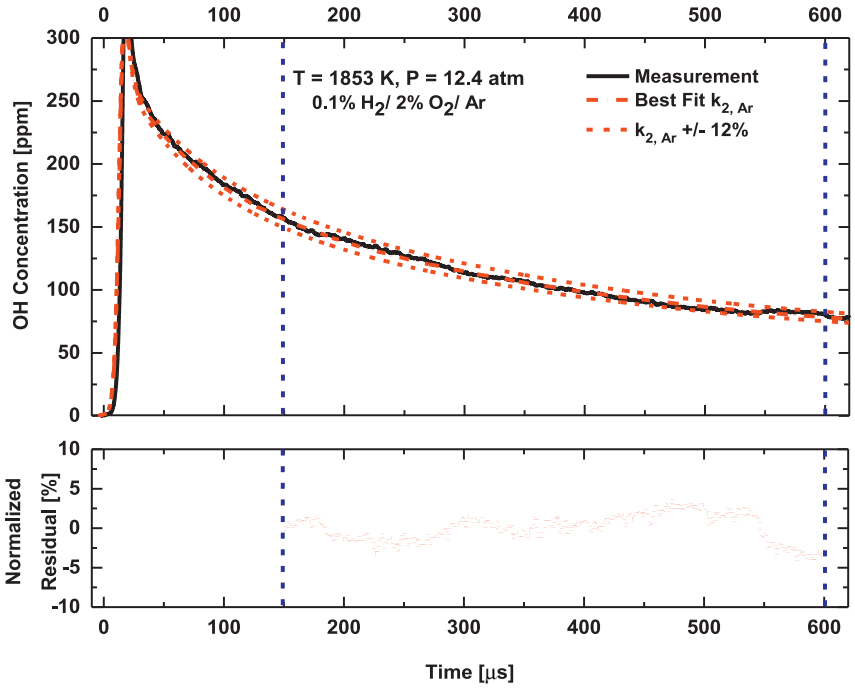

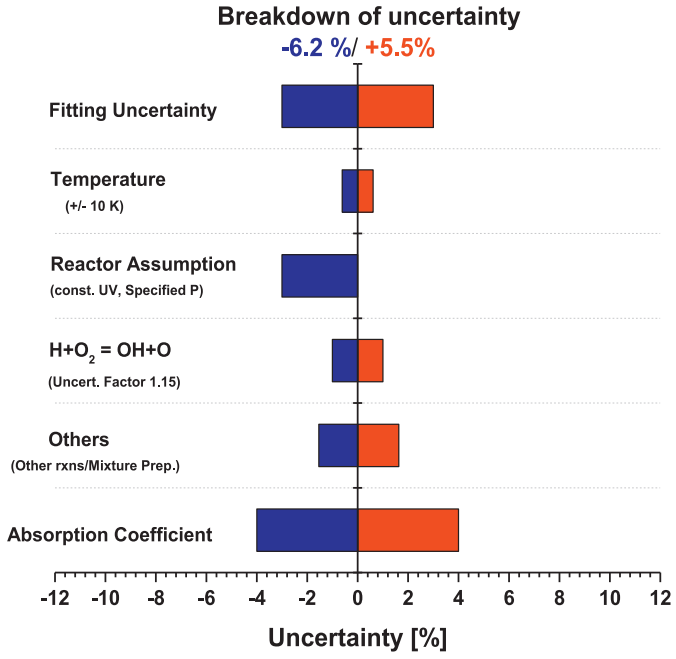

Fig. 6. (Top) Example OH trace measured behind the reflected shock at an initial temperature and pressure of 1853 K, 12.4 atm respectively, for the test mixture 0.1% H_2/ O_2/ Ar. Simulations performed using the modified FFCM-1 mechanism with the best-fit rate coefficient for $k_{2,Ar}$ and perturbations of ±12% are shown in red (Bottom) Uncertainty breakdown for the measurement of $k_{2,Ar}$. (For interpretation of the references to color in this figure legend, the reader is referred to the web version of this article.)

magnitude depended on well-known thermochemical parameters (i.e. $\Delta_f H°_{298}$ per Ruscic et al. [42]). To characterize the linestrength and lineshape completely, ~ 8 shocks were conducted at a repeated condition—tuning the laser to a different wavelength for each—to generate a sufficient survey of the absorption profile (see Fig. 4). The details of this lineshape characterization process, specifically for Argon and Nitrogen as collision partners, can be found in Girard et al. [31]; relevant results are included in Table 1.

The characterization of the CO_2-broadened lineshape was conducted similarly to that of Argon and Nitrogen [31], but due to significant beam-steering noise beyond ~200 μs, the peak magnitude was used in place of the plateau value as a more repeatable measure of relative OH concentration. The values for the O_2, N_2, and Ar-broadened parameters have been published by Shirinzadeh et al. [43], referenced to room temperature. Despite the large uncertainty in extrapolating these parameters to high temperatures, they agreed with the current study for Ar and N_2 broadening; therefore, the parameters associated with O_2 were deemed adequately precise for this study. Considering the low concentrations of O_2 used in the driven mixtures (typically less than 5%) for this study, the high uncertainty in the extrapolated

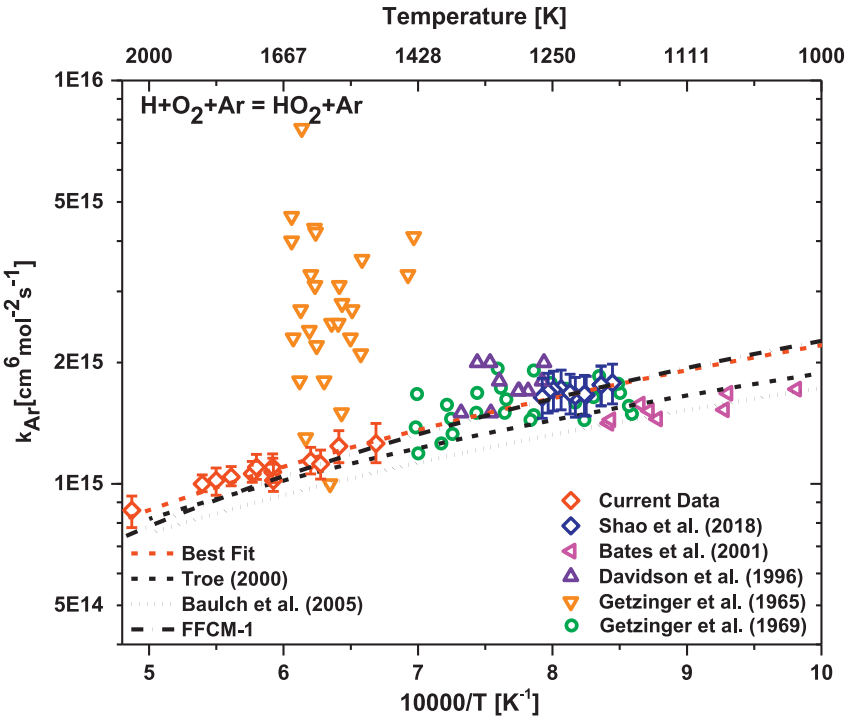

Fig. 7. Arrhenius plot for $H+O_2+Ar=HO_2+Ar$ comparing the current measurements with selected previous works in the temperature range of 1000–2000 K.

Table 3
List of experiments.

S. No.	Temperature (K)	Pressure (atm)	Rate ($cm^6mol^{-2}s^{-1}$)	Uncertainty (%) −	+
ARGON	Mixture:	0.1% H_2/ 2% O_2/ Ar			
1	1689	16.18	1.07E + 15	7.74	7.90
2	1734	15.84	1.06E + 15	6.76	7.12
3	1782	14.75	1.04E + 15	5.46	7.21
4	1690	16.20	1.10E + 15	7.34	8.70
5	2053	11.78	8.60E + 14	8.00	10.79
6	1819	12.80	1.02E + 15	6.82	9.72
7	1853	12.40	1.00E + 15	6.20	5.54
8	1725	12.97	1.10E + 15	7.05	6.27
9	1688	13.71	1.02E + 15	9.36	8.06
10	1613	13.66	1.14E + 15	7.64	8.89
11	1593	14.01	1.12E + 15	7.83	9.76
12	1560	14.41	1.24E + 15	8.85	10.43
13	1495	14.68	1.26E + 15	11.76	11.73
NITROGEN	Mixture:	0.1% H_2/ 2% O_2/ N_2			
1	1839	20.1	9.32E + 14	20.27	20.06
2	1834	20	9.75E + 14	23.85	15.25
3	1908	18.84	9.42E + 14	11.24	18.22
4	1812	20.97	9.15E + 14	21.64	32.99
5	1761	21.68	9.38E + 14	12.29	23.26
6	1702	9.35	9.92E + 14	18.46	28.18
7	1650	9.94	1.15E + 15	17.61	22.63
8	1554	10.61	1.25E + 15	16.81	25.73
9	1552	11.55	1.40E + 15	19.40	25.38
CARBON DIOXIDE	Mixture:	0.1% H_2/ 6% O_2/ 10% CO_2/ Ar			
1	1688	13.27	6.20E + 15	28.29	28.39
2	1546	13.91	7.00E + 15	24.8	23.2
3	1486	14.09	7.50E + 15	30.72	29.96
4	1650	13.36	5.40E + 15	25.41	27.17
5	1568	13.45	6.40E + 15	26.75	27.29

O_2-broadened parameters from Shirinzadeh et al. [43] was not problematic.

Table 2 presents the 1-σ uncertainties of the primary spectroscopic error sources (i.e. those that contributed over 0.1%) involved in the OH measurements after applying the calculated spectral parameters. In the error analysis, all listed sources were considered as independent and 1-σ error was estimated for each. Subsequently, their contributions to measured OH mole fraction error were estimated through Monte-Carlo simulation, insuring adequately sized sets sampled from normal distributions of each error source. The broadening and shift uncertainties include the typical error introduced in converting from the reference temperature value to a given condition, using measured temperature-dependence coefficients for Ar and N_2 [31] and estimated values from Herbon [36] and collisional theory [30] for O_2 and CO_2.

3. Rate constant determination methodology

The experimentally obtained OH time-histories were best-fit with simulated OH traces to estimate $k_{2,M}$. FFCM-1 was used as the reference mechanism for the simulations. The time-interval during which the sensitivity of OH to the reaction R2 is maximum, almost flat, and lies within the facility test time, was chosen as the region for determining the best fit. From Fig. 1, this interval ranges from 150 µs to 600 µs for M = Ar. Sensitivity analysis, performed with N_2, and CO_2 as collision partners, also confirms that the chosen time-interval also works for M = N_2, CO_2. For experiments where the test time (limited by contact surface arrival) was lower than the aforementioned time-interval, the interval throughout which the pressure trace remained flat was chosen.

A detailed uncertainty analysis was conducted for each experiment and is shown along with the corresponding measured and fitted traces in the subsequent sections. The sources of uncertainty considered in the analysis include the effect of other reactions, temperature, absorption coefficient of OH, deviation of the behavior of the shock tube from that of a constant volume/constant pressure reactor, and uncertainty in the composition of the prepared mixture. To determine the impact of other reactions, the rate constant of each of the contributing reactions was individually perturbed by its quoted uncertainty factor, while keeping everything else constant. The least-square-fit procedure was repeated to determine k_2 with the perturbed secondary reaction. Similar methodology was used to determine the uncertainty in k_2 due to the uncertainty in the OH absorption coefficient. The uncertainty from the initial temperature was estimated by the theory of propagation of uncertainty using an Arrhenius expression obtained from the measurements.

Shock tubes can be ideally modeled as a constant volume reactor, or as a constant pressure reactor. These two idealizations serve as bounds for the actual conditions within a shock tube during the test time. To determine the effect of this deviation on k_2, simulated OH time-histories were generated using constrained-UV, constrained-HP, and with specified pressure profiles (measured by the pressure transducers) for each experiment. Each of these traces was best-fit with the measured trace to determine the uncertainty in k_2 due to the reactor assumption chosen for simulating the traces. The overall 2-σ uncertainty was determined by taking the root mean-squared value of the individual uncertainties.

4. Results and discussions

4.1. $H + O_2 + Ar = HO_2 + Ar$

A total of 12 experiments were conducted in the temperature range of 1450–2000 K. The pressure was in the range of 10–22 atm. Prior to the experiments, the shock tube was thoroughly cleaned following standard procedures [44]. Post cleaning, a non-reacting shock was run at a temperature higher than 2000 K to check for formation of OH radicals from any remaining impurities. The pressure and laser signals recorded from one such non-reacting experiment is shown in Fig. 5. The laser intensity remains unchanged throughout the test time, which confirms the absence of OH radicals. Also shown in Fig. 5 is a raw absorbance trace obtained from one of the reacting experiments. The absorbance during most of the fitting interval is between 0.5 and 1, which ensures a high signal to noise ratio (SNR) for the test conditions.

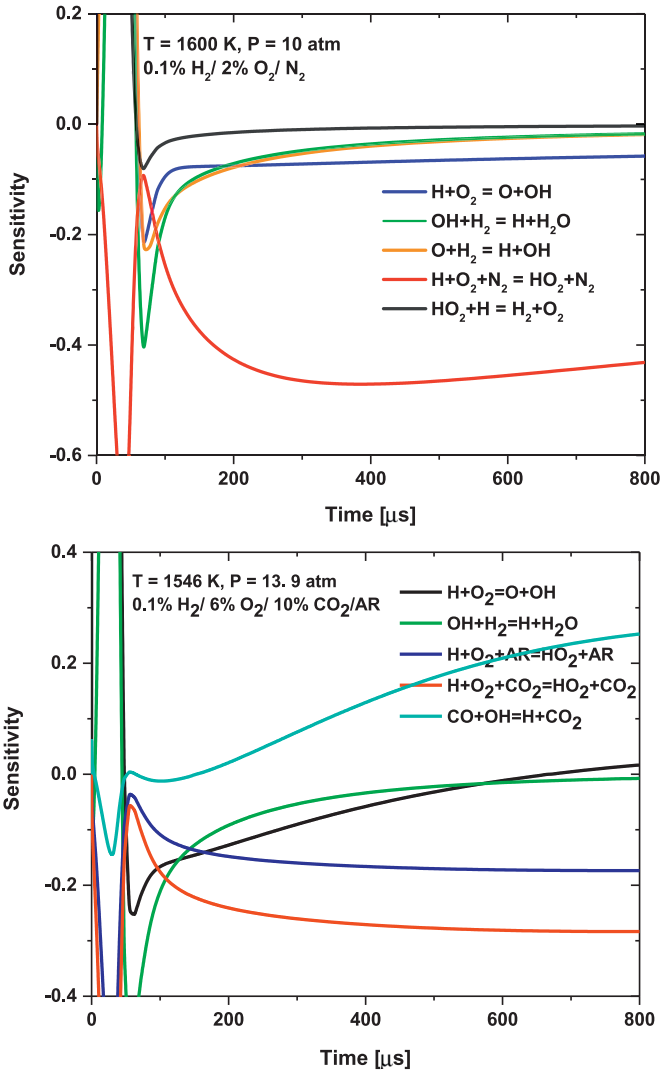

Fig. 8. Sensitivity analysis of OH time-history during lean oxidation of Hydrogen with (top) Nitrogen as the bath gas, and (bottom) Carbon Dioxide/Argon as the bath gas.

The measured OH trace, along with the best-fit simulated trace for one of the test conditions is shown in Fig. 6. The OH trace obtained by perturbing $k_{2,\,AR}$ by +/− 12% is also shown in Fig. 6 to illustrate the sensitivity of the OH trace to R2. The difference between the simulation and the measurement, normalized by the measured OH concentration at each time-step is defined as the residual, and is expressed as a percentage within the fitting interval in Fig. 6. Minimization of the sum of the square of residuals over the fitting time-interval was used as the metric to determine the best fit k_2. Figure 6 also shows the detailed breakdown of uncertainty for the above discussed test condition. The major contribution to the uncertainty comes from the uncertainty in the absorption coefficient (+/−4%).

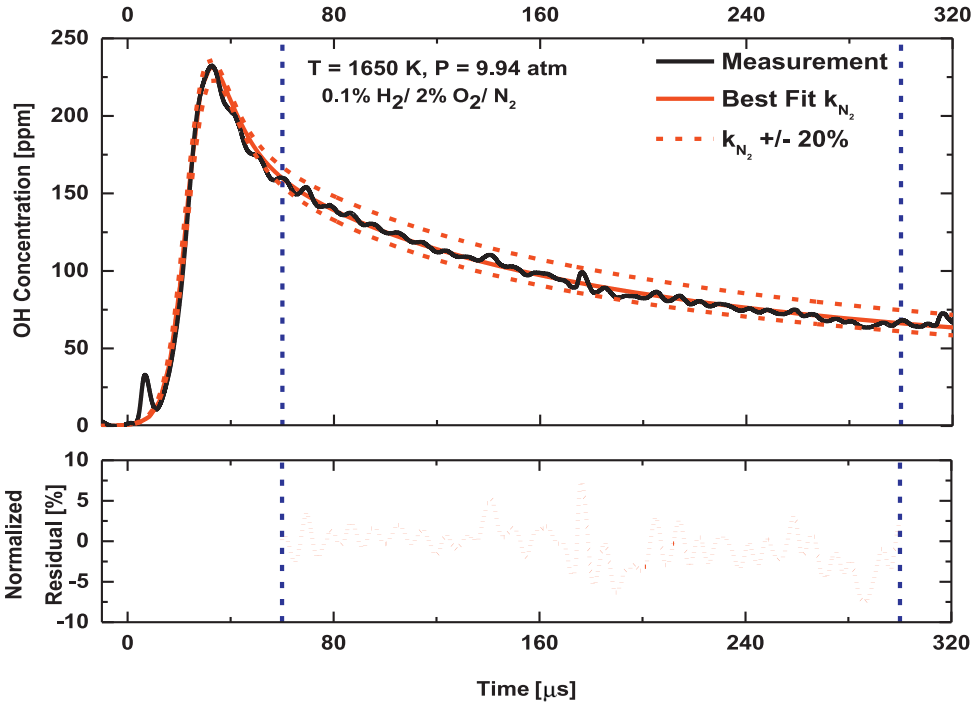

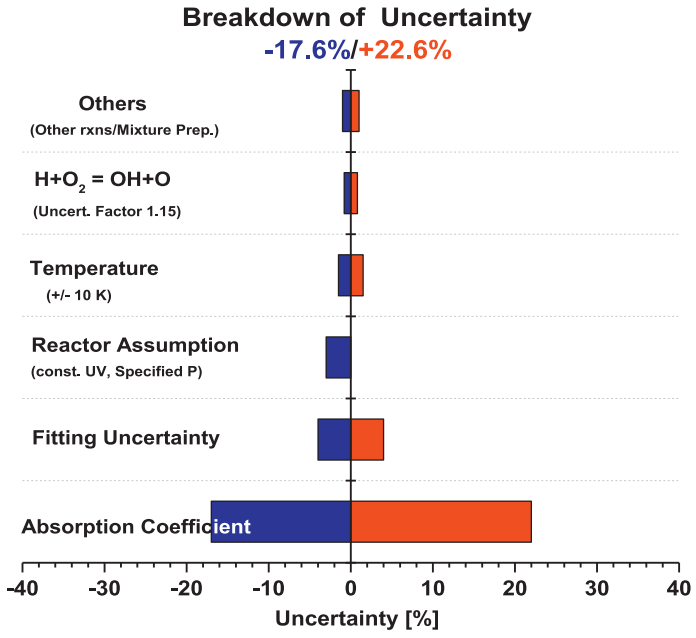

Fig. 9. (Top) Example OH trace measured behind the reflected shock at an initial temperature and pressure of 1650 K, 9.94 atm, for the test mixture 0.1% H_2/ 2% O_2/ N_2. Simulations performed using the modified FFCM-1 mechanism with the best-fit rate coefficient for k_{2,N_2} and perturbations of ±20% are shown in red. (Bottom) Uncertainty breakdown for the measurement of k_{2,N_2}.

The breakdown of the uncertainty in the absorption coefficient is discussed in Section 2.3.2 and summarized in Table 2. The absorption coefficient is a function of the linestrength and the lineshape. Lineshape is a function of both pressure, and temperature, while the linestrength is dependent on temperature. Thus, the uncertainty in the measured values of pressure and temperature also propagates to the absorption coefficient through the linestrength and the lineshape.

The measured values of $k_{2,AR}$ show a weak temperature dependence, as shown in Fig. 7. Therefore, the effect of the uncertainty in the temperature behind the reflected shock, on the rate constant is low (~1%). The contribution of R1 to the overall uncertainty is also small (~1%). R1 was the reaction with the second highest sensitivity at the chosen conditions, which itself was very small. The influence of uncertainty in the rate constants of other reactions, and uncertainty in the mixture preparation contributed +/−2% to the overall uncertainty. The resulting overall uncertainty for this case, at 1853 K was calculated to be ~−6.2%/+5.5%. The uncertainty is higher at temperatures greater than 1900 K, owing to the decrease in the absolute sensitivity of the OH time-history to R2. The measured rate constant, and uncertainty bounds for each of the experiments are tabulated in Table 3.

The measurements show good agreement with previous investigations at lower temperatures, within their respective uncertainties. Therefore, a common correlation that best-fits both sets of data can be used reliably with the mechanisms over a wider temperature range. Using the recently reported Stanford data at lower temperatures by Shao et al. [9], and the high-temperature data reported in this work, the best fit rate constant expression obtained, is given by

$$k_{2,Ar} = \left(2.66 * 10^{19}\right) * T^{-1.36}\ \mathrm{cm^6 mol^{-2} s^{-1}}\ (+/-9\,\%)$$

The R^2 for the fit was 0.91, and the overall 2-σ uncertainty was found to be +/−9%. The current measurements exhibit significantly less scatter, and lower uncertainties at high temperatures than earlier studies. We believe also that this is the first reported measurement of this reaction rate at temperatures greater than 1700 K. The best-fit rate constant expression agrees reasonably well with FFCM-1, the theoretical calculations of Troe [21], and recommendations of Baulch et al. [45].

It should be noted that using an alternative mechanism to reduce the data results in a slightly different rate constant determination, which agrees with the rates determined using FFCM-1 within the quoted uncertainty. If the ARAMCO 2.0 model [46] is used as the base mechanism for simulations, a lower value of $k_{2,\,Ar}$ is recovered than found with the FFCM-1 model (~8% lower) (with the same uncertainty). This difference is related to the different values used in the two mechanisms for the rate constants for R1, R11 (uncertainty factor of 1.6), and R12(uncertainty factor of 1.2).

$$O + H_2 = H + OH \qquad (R11)$$

$$OH + H_2 = H + H_2O \qquad (R12)$$

These three reactions play an important role in determining the OH concentration during the induction time, and immediately after ignition. ARAMCO 2.0 uses the rate constant expression suggested by Hong et al. [7] for R1, while FFCM-1 uses the rate constant expression which was slightly modified by an optimization procedure outlined by Tao et al. [47]. For the reaction R11, FFCM-1 uses the rate constant expression recommended in the recent review by Baulch et al. [45], which shows excellent agreement with measurements reported over a wide temperature range. On the contrary, ARAMCO 2.0 uses the rate constant expression determined by Sutherland et al. [48], which was not used in the Baulch review in favor of a rate constant expression that improves fit over lower temperature data. For R12, ARAMCO 2.0 uses the rate constant expression suggested by Lam et al. [49], while FFCM-1 uses the rate constant reported by Sutherland et al. The measurements of Lam et al. show much less scatter, and lower uncertainty, but their experiments were carried out at a temperature lower than the experiments of Michael et al. [50]. Owing to the reasons outlined above, FFCM-1 was the preferred base mechanism for this study. It should be noted that the uncertainty analysis performed for $k_{2,\,Ar}$ individually accounts for the contribution from other reactions, which implicitly accounts for the uncertainty stemming from the choice of the base mechanism.

4.2. $H + O_2 + N_2 = HO_2 + N_2$

For determining k_{2,N_2}, a mixture with same dilution and equivalence ratio was used with the bath gas being Nitrogen instead Argon. In Fig. 8, sensitivity analysis of the OH time-history for this mixture at one of the representative conditions shows the post-ignition dominance of R2. Among the other reactions that show up in the sensitivity plot at longer times, R1 is most important. The sensitivity is dominated by R2 over the temperature range of 1500–2000 K and pressures 8–30 atm. The approach used for determining the rate constant was similar to the one outlined earlier, with the fitting interval chosen to ensure maximum sensitivity to R2, within the facility test time.

Figure 9 shows the measured trace with the simulated best-fit trace, and the traces obtained by perturbing the measured rate constant by 20%. The rate constants are plotted against the inverse

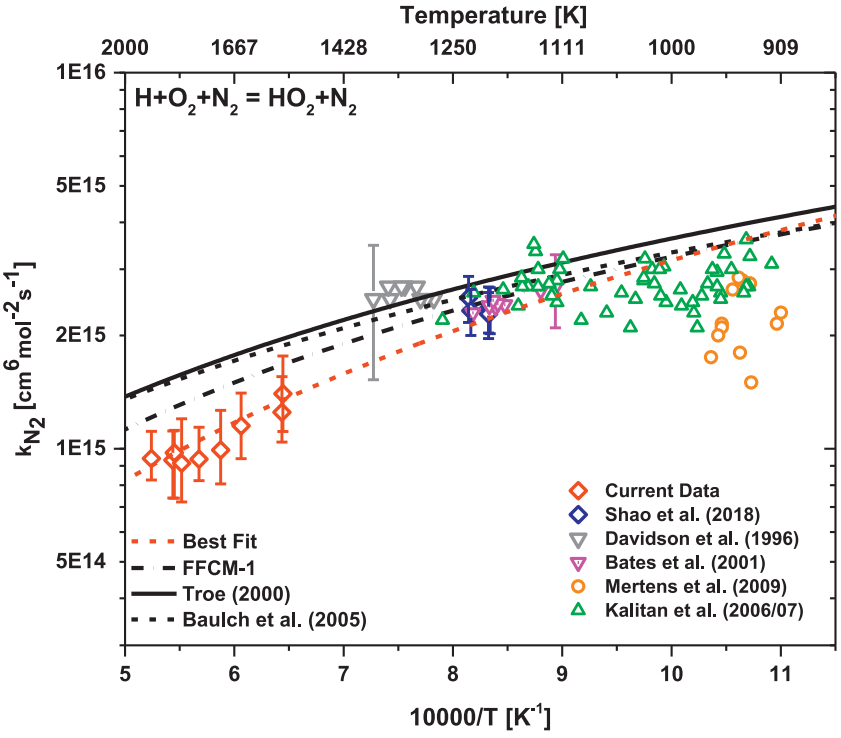

Fig. 10. Arrhenius plot for $H + O_2 + N_2 = HO_2 + N_2$ showing the current measurements and selected previous measurements in the temperature range of 900–2000 K.

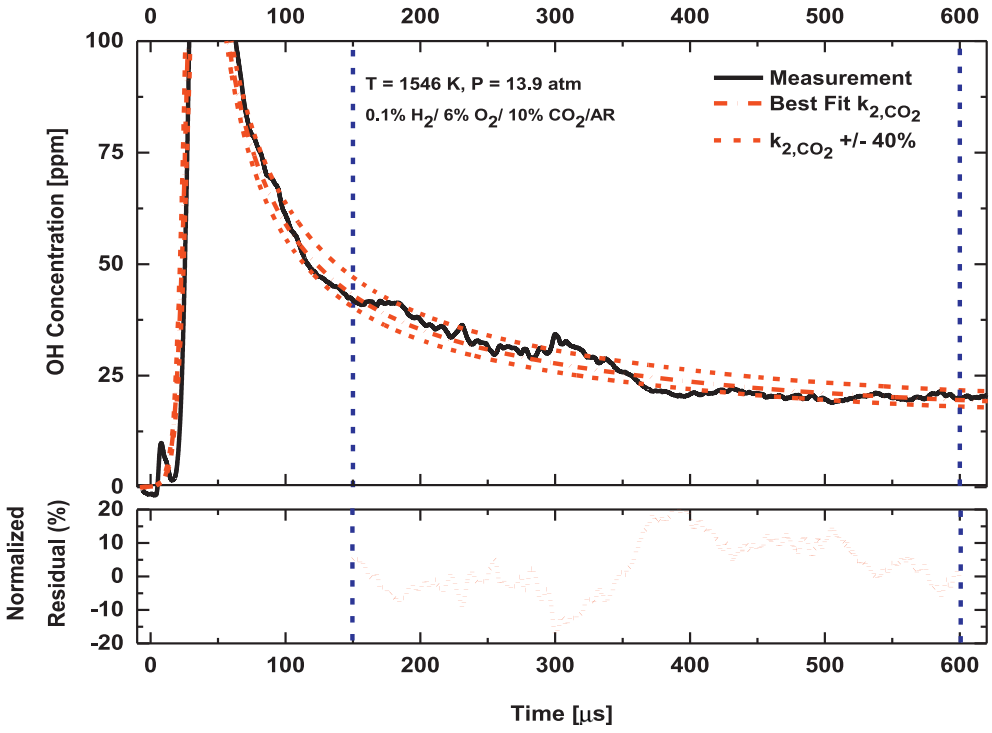

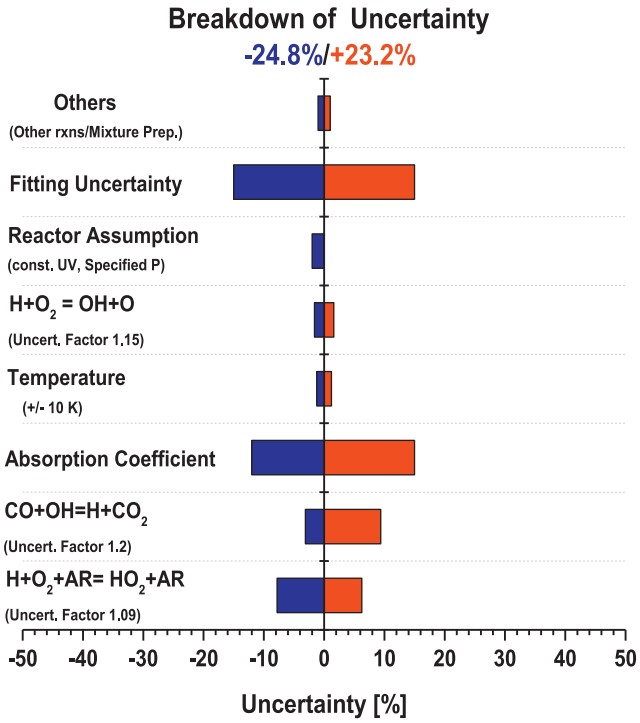

Fig. 11. (Top) Example OH trace measured behind the reflected shock at 1650 K, 9.94 atm, for the test mixture 0.1% H_2/ 2% O_2/ N_2. Simulations performed using modified FFCM-1 with best fit rate constant for $k_{2,CO2}$, with perturbations of ±20% are shown in red (Bottom) Uncertainty breakdown for the measurement of $k_{2,CO2}$. (For interpretation of the references to color in this figure legend, the reader is referred to the web version of this article.)

of temperature (see Fig. 10), along with the results available in literature. The current measurements are the only measurements of this reaction rate constant at temperatures above 1400 K. The measurements also exhibit low scatter but larger uncertainties (~+/− 23%) than were determined for $k_{2,Ar}$. The largest contribution to this uncertainty is from spectroscopic parameters. Despite the calibration measurements, the uncertainties in the broadening coefficient, and the pressure-shift parameter for Nitrogen were higher than that for Argon, which resulted in greater uncertainty in the absorption coefficient (see Table 2). The contribution from other reactions to the uncertainty was negligible. A correlation obtained using the low temperature data from Shao et al. [9], and the current high-temperature data gives the following expression for k_{2,N_2}.

$$k_{2,N_2} = \left(2.25 * 10^{21}\right) * T^{-1.95}\ \mathrm{cm^6 mol^{-2} s^{-1}} (\pm 23\ \%)$$

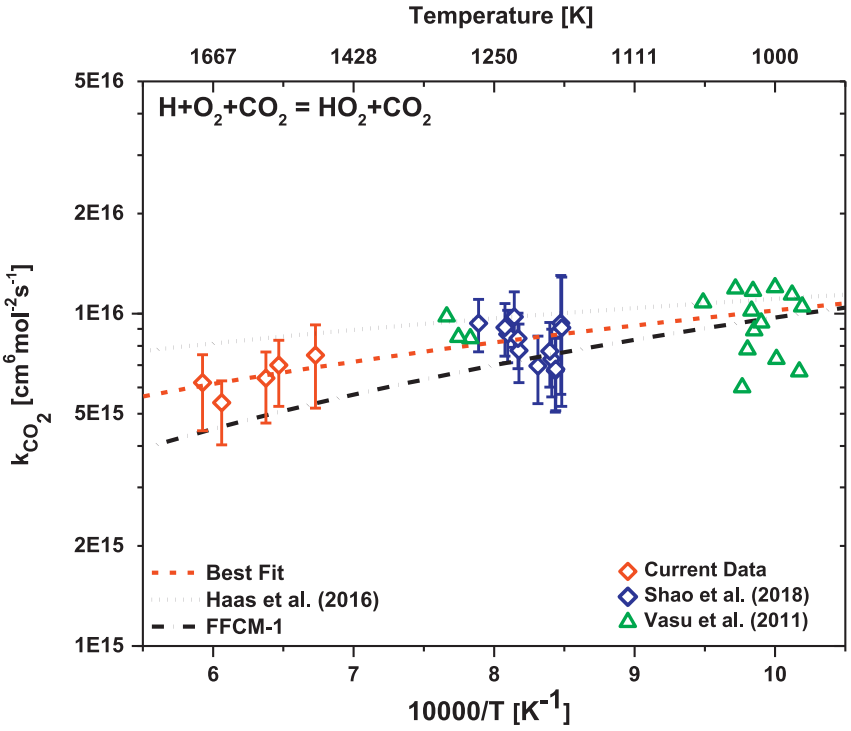

Fig. 12. Arrhenius plot for $H+O_2+CO_2=HO_2+CO_2$ showing the current measurements and selected previous measurements in the temperature range of 1000–2000 K.

The suggested correlation agrees with the low temperature measurements of Kalitan et al. [51,52], and Bates et al. [17]. Within their respective error bars, the correlation also agrees with the measurements of Davidson et al. [13], and Mertens et al. [10]. The temperature dependence of k_{N2} is slightly stronger than for $k_{2,Ar}$, which suggests a temperature dependence of the ratio of collision efficiencies of Nitrogen and Argon. This is not observed in the rate constants used in the mechanisms, which usually assume the same temperature dependence of the collision efficiencies for Ar, and N_2 [20]. The collision efficiency accounts for the weak collision effects which is a function of the average energy exchanged per collision, $<\Delta E>$ between the activated molecule and the other molecules in the mixture [53]. The data reported in this work spans a wide temperature range and can therefore be used for deducing more accurate expressions for $<\Delta E>$ and improving the theoretical model for R2.

4.3. $H+O_2+CO_2=HO_2+CO_2$

Figure 8 also shows the sensitivity analysis, performed for the OH radicals for a representative test condition for determining k_{2,CO_2}. Pure CO_2 was not used as the diluent for multiple reasons. At high concentrations of CO_2, the sensitivity of the OH radicals to R2 is lower than R10. However, it should be noted that R10 is well known and Joshi et al. [54] have reported the high-temperature rate constant for R10 with an uncertainty factor of 1.2. Thus, despite its significance at the chosen test conditions its contribution to the overall uncertainty is not very high. The OH time-history is also sensitive to $R2_{Ar}$, as seen from Fig. 8. Since the rate constant of $R2_{Ar}$ has been already determined well, within 9% uncertainty, as described in the previous section, the effect on the uncertainty is not prohibitively large.

The sensitivity of OH to R2 is also dependent on the concentration of CO_2 in the mixture for a given temperature. At temperatures higher than 1400 K, the available shock tube test time is significantly reduced when the driven gas has a high concentration of CO_2. Using 10% CO_2/Ar as the test mixture ensured high-sensitivity of OH to R2, while leading to a test time of ~800 μs. An example trace is shown in Fig. 11, with the corresponding uncertainty breakdown. The Arrhenius plot for k_{2,CO_2} is shown in Fig. 12. Within the quoted uncertainties, the measurements agree with the low-temperature measurements of Shao et al. [9], and Vasu et al. [55]. The expression for the rate constant obtained by fitting the current measurements, and the low-temperature data by Shao et al. [9] is given by

$$k_{2,CO_2} = \left(2.233 * 10^{18}\right) * T^{-0.79}\ \mathrm{cm^6 mol^{-2} s^{-1}} (\pm 28\%)$$

The measured rate constant shows a slightly stronger temperature dependence than the recommendation by Haas [56], which was based on a reassessment of existing literature data combined with flow reactor measurements.

$$k_{2,CO_2,Haas} = \left(10^{17.86\pm0.68}\right) * T^{-0.605\pm0.179}\ \mathrm{cm^6 mol^{-2} s^{-1}}$$

The major contribution to the uncertainty is from the uncertainty in fitting the measured OH time-history (~+15%), uncertainty in the knowledge of the absorption coefficient/spectroscopy (~+/−15%). R2 and R10 also contribute significantly to the overall uncertainty. The effect of temperature and other reactions is small (~1% each). The overall uncertainty in k_{2,CO_2} is +/−28%, which is comparable to the uncertainty reported by Shao et al. [9].

5. Conclusions

The rate constants of $H+O_2+M=HO_2+M$ near the low pressure limit was measured for three bath gases (Argon, Nitrogen, and Carbon Dioxide) between 1450 K and 2000 K. Lean oxidation of Hydrogen renders the OH radical time-history to be dominantly sensitive to the title reactions at these temperatures. Fitting the OH traces, measured using a sensitive laser absorption diagnostic, with simulated traces allowed for the determination of the reaction rate constant. The combined fit of the current results with the measurements of Shao et al. at lower temperatures, was used to obtain rate constant expressions for all three bath gases.

$$k_{2,Ar} = \left(2.66x10^{19}\right) * T^{-1.36}\ \mathrm{cm^6 mol^{-2} s^{-1}}\ (\pm 9\ \%)$$

$$k_{2,N_2} = \left(2.25x10^{21}\right) * T^{-1.95}\ \mathrm{cm^6 mol^{-2} s^{-1}} (\pm 23\%)$$

$$k_{2,CO_2} = \left(2.23x10^{18}\right) * T^{-0.79}\ \mathrm{cm^6 mol^{-2} s^{-1}} (\pm 28\%)$$

The rate constant expressions show good agreement with all available data within the combustion relevant temperature range of 800–2000 K. The current dataset is the first reported measurement of these reaction rates constant beyond 1700 K, and exhibits low scatter, with low uncertainties.

Acknowledgment

This work was supported by the Air Force Office of Scientific Research through AFOSR Grant No. FA9550-16-1-0195, with Chiping Li as contract monitor.

References

[1] M. Mehl, W.J. Pitz, C.K. Westbrook, H.J. Curran, Kinetic modeling of gasoline surrogate components and mixtures under engine conditions, Proc. Combust. Inst. 33 (2011) 193–200.
[2] A. Kéromnès, W.K. Metcalfe, K.A. Heufer, N. Donohoe, A.K. Das, C.J. Sung, J. Herzler, C. Naumann, P. Griebel, O. Mathieu, M.C. Krejci, An experimental and detailed chemical kinetic modeling study of hydrogen and syngas mixture oxidation at elevated pressures, Combust. Flame 160 (6) (2013) 995–1011.
[3] H. Wang, R. Xu, K. Wang, C.T. Bowman, R.K. Hanson, D.F. Davidson, K. Brezinsky, F.N. Egolfopoulos, A physics-based approach to modeling real-fuel combustion chemistry-I. Evidence from experiments, and thermodynamic, chemical kinetic and statistical considerations, Combust. Flame 193 (2018) 502–519.
[4] E.L. Ranzi, A. Frassoldati, R. Grana, A. Cuoci, T. Faravelli, A.P. Kelley, C.K. Law, Hierarchical and comparative kinetic modeling of laminar flame speeds of hydrocarbon and oxygenated fuels, Prog. Energy Combust. Sci. 38 (2012) 468–501.
[5] L. Cai, H. Pitsch, Optimized chemical mechanism for combustion of gasoline surrogate fuels, Combust. Flame 162 (2015) 1623–1637.
[6] Y. Tao, G.P. Smith, H. Wang, Critical kinetic uncertainties in modeling hydrogen/carbon monoxide, methane, methanol, formaldehyde, and ethylene combustion, Combust. Flame 195 (2018) 18–29.
[7] Z. Hong, D.F. Davidson, E.A. Barbour, R.K. Hanson, A new shock tube study of the H+ O_2→ OH+ O reaction rate using tunable diode laser absorption of H_2O near 2.5 μm, Proc. Combust. Inst. 33 (1) (2011) 309–316.
[8] S. Wang, D.F. Davidson, R.K. Hanson, Shock tube and laser absorption study of CH_2O oxidation via simultaneous measurements of OH and CO, J. Phys. Chem. A 121 (45) (2017) 8561–8568.
[9] J. Shao, R. Choudhary, A. Susa, D.F. Davidson, R.K. Hanson, Shock tube study of the rate constants for H+ O_2+ M→ HO_2+ M (M= Ar, H_2O, CO_2, N_2) at elevated pressures, Proc. Combust. Inst. 37 (1) (2019) 145–152.
[10] J.D. Mertens, D.M. Kalitan, A.B. Barrett, E.L. Petersen, Determination of the rate of H+ O_2+ M→ HO_2+ M (M= N_2, Ar, H_2O) from ignition of syngas at practical conditions, Proc. Combust. Inst. 32 (1) (2009) 295–303.
[11] R.W. Getzinger, G.L. Schott, Kinetic studies of hydroxyl radicals in shock waves. V. recombination via the H+ O_2+ M→ HO_2+ M reaction in lean hydrogen—oxygen mixtures, J. Chem. Phys. 43 (9) (1965) 3237–3247.
[12] L.S. Blair, R.W. Getzinger, A shock tube study of recombination in the hydrogen-oxygen reaction using infrared emission from water vapor, Combust. Flame 14 (1) (1970) 5–12.
[13] D.F. Davidson, E.L. Petersen, M. Röhrig, R.K. Hanson, C.T. Bowman, Measurement of the rate coefficient of H+ O_2+ M→ HO_2+ M for M= Ar and N_2 at high pressures, Symp. (Int.) Combust. 26 (1) (1996) 481–488.
[14] J.H. Bromly, F.J. Barnes, P.F. Nelson, B.S. Haynes, Kinetics and modeling of the H_2/O_2/NOx system, Int. J. Chem. Kinet. 27 (12) (1995) 1165–1178.
[15] P.J. Ashman, B.S. Haynes, Rate coefficient of H+ O_2+ M→ HO_2+ M (M= H_2O, N_2, Ar, CO_2), Symp. (Int.) Combust. 27 (1) (1998) 185–191.
[16] M.A. Mueller, R.A. Yetter, F.L. Dryer, Flow reactor studies and kinetic modeling of the H_2/O_2/NOx and CO/H_2O/O_2/NOx reactions, Int. J. Chem. Kinet. 31 (10) (1999) 705–724.
[17] R.W. Bates, D.M. Golden, R.K. Hanson, C.T. Bowman, Experimental study and modeling of the reaction H+ O_2+ M→ HO_2+ M (M= Ar, N_2, H_2O) at elevated pressures and temperatures between 1050 and 1250 K, Phys. Chem. Chem. Phys. 3 (12) (2001) 2337–2342.
[18] R.X. Fernandes, K. Luther, J. Troe, V.G. Ushakov, Experimental and modelling study of the recombination reaction H+ O_2 (+ M)→ HO_2 (+ M) between 300 and 900 K, 1.5 and 950 bar, and in the bath gases M= He, Ar, and N_2, Phys. Chem. Chem. Phys. 10 (2008) 4313–4321.
[19] S. Wang, R.K. Hanson, High-sensitivity 308.6-nm laser absorption diagnostic optimized for OH measurement in shock tube combustion studies, Appl. Phys. B 124 (3) (2018) 37.
[20] G.P. Smith, Y. Tao, H. Wang, Foundational fuel chemistry model version 1.0 (FFCM-1). http://nanoenergy.stanford.edu/ffcm1, 2016.
[21] J. Troe, Detailed modeling of the temperature and pressure dependence of the reaction H+ O_2 (+ M)→ HO_2 (+ M), Proc. Combust. Inst. 28 (2) (2000) 1463–1469.
[22] S.R. Sellevåg, Y. Georgievskii, J.A. Miller, The temperature and pressure dependence of the reactions H+ O_2 (+ M)→ HO_2 (+ M) and H+ OH (+ M)→ H_2O (+ M), J. Phys. Chem. A 112 (2008) 5085–5095.
[23] Z. Hong, D.F. Davidson, R.K. Hanson, An improved H_2/O_2 mechanism based on recent shock tube/laser absorption measurements, Combust. Flame 158 (4) (2011) 633–644.
[24] J. Urzay, N. Kseib, D.F. Davidson, G. Iaccarino, R.K. Hanson, Uncertainty-quantification analysis of the effects of residual impurities on hydrogen–oxygen ignition in shock tubes, Combust. Flame 161 (1) (2014) 1–15.
[25] J. Shao, Y. Zhu, S. Wang, D.F. Davidson, R.K. Hanson, A shock tube study of jet fuel pyrolysis and ignition at elevated pressures and temperatures, Fuel 226 (2018) 338–344.
[26] J. Shao, D.F. Davidson, R.K. Hanson, A shock tube study of ignition delay times in diluted methane, ethylene, propene and their blends at elevated pressures, Fuel 225 (2018) 370–380.
[27] J. Shao, R. Choudhary, D.F. Davidson, R.K. Hanson, S. Barak, S.S. Vasu, Ignition delay times of methane and hydrogen highly diluted in carbon dioxide at high pressures up to 300 atm, Proc. Combust. Inst. 37 (4) (2019) 4555–4562.
[28] D.F. Davidson, J.K. Shao, R. Choudhary, M. Mehl, N. Obrecht, R.K. Hanson, Ignition delay time measurements and modeling for gasoline at very high pressures, Proc. Combust. Inst. 37 (4) (2019) 4885–4892.
[29] A.G. Gaydon, I.R. Hurle, The shock tube in high-temperature chemical physics Reinhold, 1963).
[30] R.K. Hanson, M.R. Spearrin, C.S. Goldenstein, Spectroscopy and optical diagnostics for gases, Springer International Publishing, 2016.
[31] J.J. Girard, R. Choudhary, R.K. Hanson, Collisional-induced broadening and shift parameters of OH with Ar and N2 near 308.6 nm, measured at T= 1300–2000 K and P= 20-100 atm, J. Quant. Spectrosc. Radiat. Transf. 221 (2018) 194–201.
[32] T.R. Meyer, S. Roy, T.N. Anderson, J.D. Miller, R.V. Katta, R.P. Lucht, R.J. Gord, Measurements of OH mole fraction and temperature up to 20 kHz by using a diode-laser-based UV absorption sensor, Appl. Opt. 44 (31) (2005) 6729–6740.
[33] M.A. Oehlschlaeger, D.F. Davidson, J.T. Herbon, R.K. Hanson, Shock tube measurements of branched alkane ignition times and OH concentration time histories, Int. J. Chem. Kinet. 36 (2004) 67–78.
[34] V. Vasudevan, D.F. Davidson, R.K. Hanson, Shock tube measurements of toluene ignition times and OH concentration time histories, Proc. Combust. Inst. 30 (2005) 1155–1163.
[35] S.S. Vasu, D.F. Davidson, Z. Hong, V. Vasudevan, R.K. Hanson, n-dodecane oxidation at high-pressures: measurements of ignition delay times and OH concentration time-histories, Proc. Combust. Inst. 32 (2009) 173–180.
[36] J.T. Herbon, Shock tube measurements of CH_3+O_2 kinetics and the heat of formation of the OH radical, Stanford University, 2004.
[37] R.K. Hanson, S. Salimian, G. Kychakoff, R.A. Booman, Shock-tube absorption measurements of OH using a remotely located dye laser, Appl. Opt. 22 (5) (1983) 641–643.
[38] A.Y. Chang, E.C. Rea, R.K. Hanson, Temperature measurements in shock tubes using a laser-based absorption technique, Appl. Opt. 26 (1987) 885–891.
[39] E.C. Rea, A.Y. Chang, R.K. Hanson, Shock-tube study of pressure broadening of the A2Σ+− X2Π (0,0) band of OH by Ar and N_2, J. Quant. Spectrosc. Radiat. Transf. 37 (2) (1987) 117–127.
[40] D.F. Davidson, M. Roehrig, E.L. Petersen, M.D. Di Rosa, R.K. Hanson, Measurements of the OH A-X (0, 0) 306 nm absorption bandhead at 60 atm and 1735 K, J. Quant. Spectrosc. Radiat. Transf. 55 (1996) 755–762.
[41] A. Goldman, J.R. Gillis, Spectral line parameters for the A2Σ-X2Π(0,0) band of OH for atmospheric and high temperatures, J. Quant. Spectrosc. Radiat. Transf. 25 (2) (1981) 111–135.
[42] B. Ruscic, A.F. Wagner, L.B. Harding, R.L. Asher, D. Feller, D.A. Dixon, K.A. Peterson, Y. Song, X. Qian, C.Y. Ng, J. Liu, W. Chen, D.W. Schwenke, On the enthalpy of formation of hydroxyl radical and gas-phase bond dissociation energies of water and hydroxyl, J. Phys. Chem. A 106 (11) (2002) 2727–2747.
[43] B. Shirinzadeh, D.M. Bakalyar, C.C. Wang, Measurement of collision induced shift and broadening of the ultraviolet transitions of OH, J. Chem. Phys. 82 (7) (1985) 2877–2879.
[44] G.A. Pang, Experimental determination of rate constants for reactions of the hydroxyl radical with alkanes and alcohols, Stanford University, 2012.
[45] D.L. Baulch, C.T. Bowman, C.J. Cobos, R.A. Cox, T. Just, J.A. Kerr, M.J. Pilling, D. Stocker, J. Troe, W. Tsang, R.W. Walker, J. Warnatz, Evaluated kinetic data for combustion modeling: supplement II, J. Phys. Chem. Ref. Data 34 (3) (2005) 757–1397.
[46] C.W. Zhou, Y. Li, E. O'Connor, K.P. Somers, S. Thion, C. Keesee, O. Mathieu, E.L. Petersen, T.A. DeVerter, M.A. Oehlschlaeger, G. Kukkadapu, C.J. Sung, M. Alrefae, F. Khaled, A. Farooq, P. Dirrenberger, P.A. Glaude, F. Battin-Leclerc, J. Santner, Y. Ju, T. Held, F.M. Haas, F.L. Dryer, H.J. Curran, A comprehensive experimental and modeling study of isobutene oxidation, Combust. Flame 167 (2016) 353–379.
[47] Y. Tao, H. Wang, Joint probability distribution of Arrhenius parameters in reaction model optimization and uncertainty minimization, Proc. Combust. Inst. 37 (1) (2019) 817–824.
[48] J.W. Sutherland, J.V. Michael, A.N. Pirraglia, F.L. Nesbitt, R.B. Klemm, Rate constant for the reaction of O (3P) with H_2 by the flash photolysis—shock tube

and flash photolysis—resonance fluorescence techniques; 504K ⩽ T ⩽ 2495 K, Symp. (Int.) Combust. 21 (1) (1988) 929–941.
[49] K.Y. Lam, D.F. Davidson, R.K. Hanson, A shock tube study of H_2+ OH→ H_2O+ H using OH laser absorption, Int. J. Chem. Kinet. 45 (6) (2013) 363–373.
[50] J.V. Michael, J.W. Sutherland, Rate constants for the reactions of hydrogen atom with water and hydroxyl with hydrogen by the flash photolysis-shock tube technique over the temperature range 1246–2297 K, J. Phys. Chem. A 92 (13) (1988) 3853–3857.
[51] D.M. Kalitan, J.D. Mertens, M.W. Crofton, E.L. Petersen, Ignition and oxidation of lean CO/H_2 fuel blends in air, J. Propuls. Power 23 (6) (2007) 1291–1301.
[52] D.M. Kalitan, E.L. Petersen, J.D. Mertens, M.W. Crofton, Ignition of lean CO/H_2/Air mixtures at elevated pressures, ASME Turbo Expo 1 (2006) 389–396, doi:10.1115/GT2006-90488.
[53] J. Troe, Theory of thermal unimolecular reactions at low pressures. I. Solutions of the master equation, J. Chem. Phys. 66 (11) (1977) 4745–4757.
[54] A.V. Joshi, H. Wang, Master equation modeling of wide range temperature and pressure dependence of CO+ OH→ products, Int. J. Chem. Kinet. 38 (1) (2006) 57–73.
[55] S.S. Vasu, D.F. Davidson, R.K. Hanson, Shock tube study of syngas ignition in rich CO_2 mixtures and determination of the rate of H+ O_2+ CO_2→ HO_2+ CO_2, Energy Fuels 25 (3) (2011) 990–997.
[56] F.M. Haas, Studies of small molecule reactions foundational to combustion chemistry, including experimental measurements from a novel high pressure flow reactor, Princeton University, 2016.